Open Access

Catalysis Research

LIDSEN Publishing Inc.

Research Article

Nano Metal Oxide Frameworks (NOF): Development of New Heterogeneous Catalyst for the Synthesis of Furan Derivatives from Glucose

Rama Jaiswal [1], Melad Shaikh [2], Kalluri V. S. Ranganath [1, *]

1. Banaras Hindu University, Institute of Science, Department of Chemistry, Varanasi, India; E-Mails: ramaruby37@gmail.com; ramaruby39@gmail.com; ranganath.chem@bhu.ac.in; rangakvs@gmail.com
2. Department of Chemistry and Biochemistry, San Diego State University, USA; E-Mail: shaikhmelad@gmail.com

* **Correspondence:** Kalluri V. S. Ranganath; E-Mails: ranganath.chem@bhu.ac.in; rangakvs@gmail.com

Academic Editor: Maria Luisa Testa

Special Issue: Development of New Heterogeneous Catalysts for Biomass Conversion

Catalysis Research
2023, volume 3, issue 4
doi:10.21926/cr.2304028

Received: June 01, 2023
Accepted: November 10, 2023
Published: November 21, 2023

Abstract

A surface modification approach has prepared a nanostructured organic framework connecting two metal oxide NPs. The surface modifier attached two metal oxide NPs *via* molecular interaction to generate modular structures of fiber, rod, or sponge materials. Thus, obtained hybrid systems have been confirmed through FT-IR, TGA, PXRD, and SEM. Metal oxides such as Fe_3O_4 and MgO generated mixed materials via the surface modification approach. Thus, obtained materials have been successfully used to dehydrate biomass-derived glucose. The products HMF and subsequently partially oxidized product DFF are considered to be valuable compounds not only in fuel technology but also in the pharmaceutical industry.

Keywords

Surface modification; HMF; DFF; metal oxide organic framework; glucose; heterogeneous catalysis

1. Introduction

Surface functionalization of metal oxide nanoparticles (NPs) can improve their properties in biological, biomedical, and catalytic applications [1]. Introducing organic moiety on their surface has become a unique material that can be used in various applications in adsorption-desorption studies [2, 3]. Such a modification over the surface of metal oxide changes their environment and increases the active sites and their catalytic efficiency [4, 5]. Recently, Fe_3O_4-based NPs with surface functionalization have been evidenced for medical applications and biosensing due to their unique structural properties, such as high surface area to volume ratio and superparamagnetic behavior [6-8]. In addition, modification of metal NPs was also studied extensively using organo-sulfur compounds such as thiols disulfides, e.g., on Au, Cu, Pt, Hg, Fe, and Ag.

Moreover, the surface of Pd has been modified with amines and ammonium ions through physisorption [4-10]. Due to effective surface modification, they provide a molecular anchor, which a secondary functional group can replace. Those secondary groups can offer to interact with other molecules of suitable functionality [11]. For instance, 4-formylbenzoic acid can act as a molecular anchor at the surface of aluminum oxide for binding aromatic amines through hydrogen bonding [12].

5-hydroxymethylfurfural (5-HMF) is one of the molecules derived from biomass sources that has attracted attention due to its versatile applications in fuel and pharmaceutical industries. It can simultaneously undergo oxidation and reduction as the molecule possesses two active functional groups. Further, HMF can be converted into a partially oxidized high-value-added compound such as 2,5-diformylfuran (2,5-DFF) 5-formylfuran carboxylic acid. DFF can be used as a ligand, anti-fungal agent, furan-based biopolymer, and furan-urea resins.

Herein, we report a synthesis of organic/inorganic nanohybrid materials connecting through a linker *via* molecular welding of metal oxides. The metal oxides selected in our present case are magnetite (Fe_3O_4) and magnesium oxide (MgO), as these are easy to synthesize [13, 14] and have been used widely in catalysis and other applications. Moreover, to generate a functionalized material (electronically tunable composites), a conductor (magnetite) and an insulator (magnesium oxide) were selected and coupled. These two nano metal oxides were modified with 4-formylbenzioc acid (**L1**), 4-(aminomethyl) benzoic acid (**L2**), and (*L*)-phenylalanine (**L3**). This surface modification allows the generation of secondary functional groups on their surface (Figure 1).

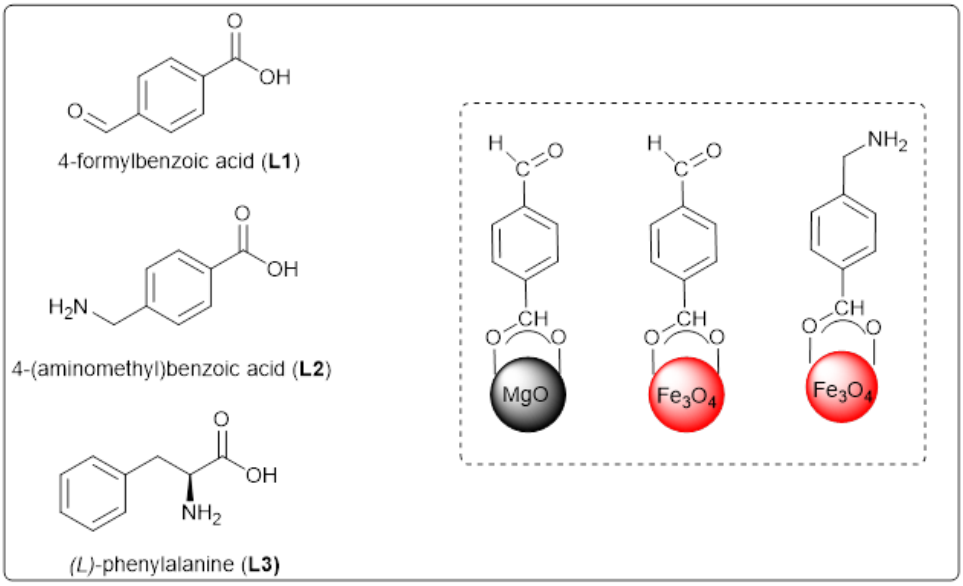

Figure 1 Surface modification of metal oxides with various ligands (black indicates magnesium oxide, and red indicates iron oxide).

Thus, obtained functional metal oxide materials have been characterized by PXRD, TGA, PXRD, TGA, and FT-IR techniques. Later, surface-modified MgO and Fe_3O_4 were utilized to generate nano-organic frameworks through covalent modification. Thus, developed -CH=N imine linkage on the surface connects two metal oxides well. It represents a new protocol using a surface modification approach to join either the same metal oxides or two different metal oxide NPs (Figure 2). Thus, nanostructured organic frameworks (NOF A, B, C, and a chiral version NOF D) have been prepared on the surface of metal oxide NPs through a surface modification approach (Figure 2). All these structurally defined materials have been characterized using powder X-ray Diffraction (PXRD), Fourier-Transform Infrared (FT-IR), elemental mapping, and Thermo Gravimetric (TGA) analysis.

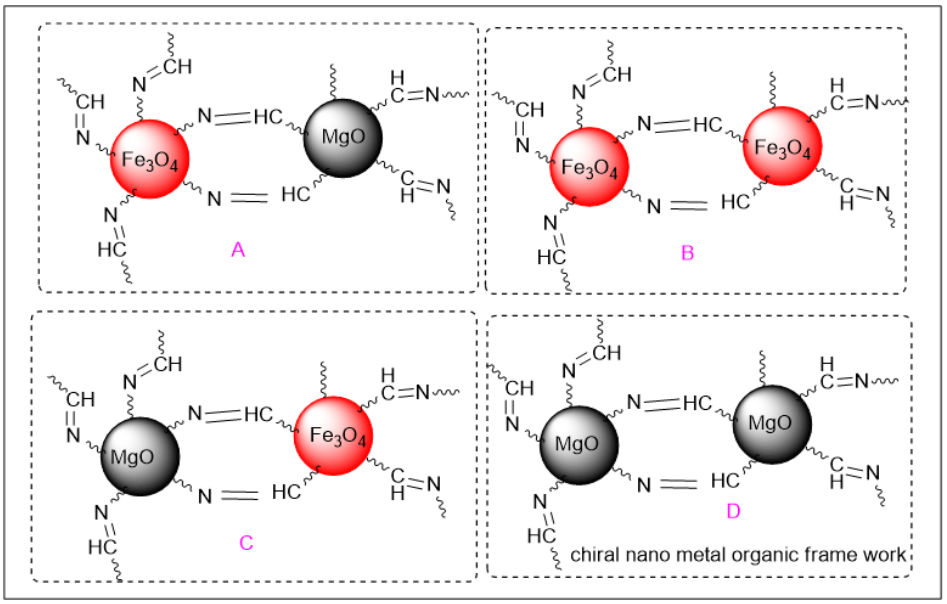

Figure 2 Nanostructured Organic Frameworks (NOFs) through Functionalization of Surface Modified Metal Oxides.

Biomass, an alternative resource for global concern-related issues in developing fuels, has been identified as a cheap raw material [15, 16]. Furan derivatives (derived from biomass) belong to such a kind of feedstock and play a vital role in biofuel technology. 5-hydroxymethyl furfural (HMF) is a bio-based platform molecule obtained from dehydration of either lignocellulosic biomass or other sources such as corn/starch [17].

The organic/inorganic hybrid materials have been explored in the dehydration of glucose by utilizing an imine framework to produce 5-hydroxymethyl furfural (HMF) and 2,5-diformylfuran (DFF), which are valuable intermediates in biofuel synthesis (Figure 3) [18-20].

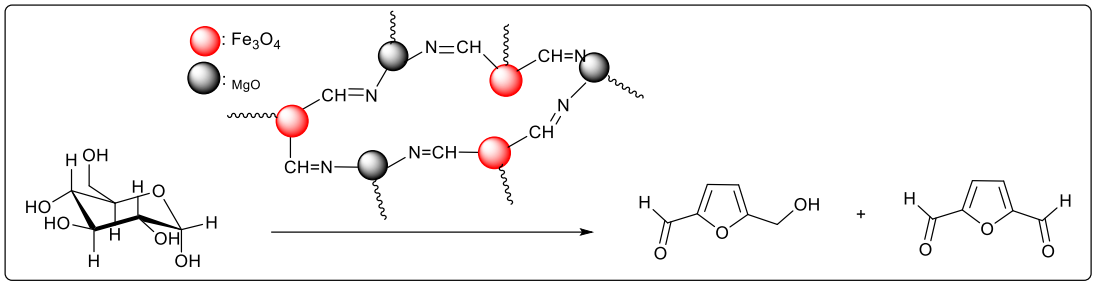

Figure 3 Application of NOFs in the decomposition of glucose.

2. Materials and Methods

2.1 Experimental

All chemicals, amines, acids, and aldehydes were purchased from Sigma-Aldrich. Initially, iron and magnesium oxide NPs were prepared, as reported by us in the previous literature [14, 21]. The nano MgO was prepared by the hydrothermal method, Fe_3O_4 was designed by the sol-gel. Powder characteristics of metal oxide and their modified materials were analyzed through high-resolution Bruker Advance (Eco)-Powder X-ray Diffractometer (PXRD) using Cu $K_{\alpha 1}$ radiation with Ni filter (Model: D8; 40 kV × 40 mA; λ = 0.1542 Å). Thermogravimetric analysis of metal oxides was done through a TG/DT analyzer (Model: STA 6000PerkinElmer, Singapore) over 30-700°C, with a temperature increment rate of 10°C/min. Surface morphology and chemical composition of active NOFs were analyzed through Scanning Electron Microscopy equipped with Energy Dispersive X-ray (SEM-EDX) (Model: FEI Quanta 250). Surface functionalization of metal oxides was also confirmed by vibration modes through JASCO Fourier-Transform Infrared (FT-IR) spectrophotometer (Model: FT/IR-4700; v: 4000-500 cm^{-1}) by preparing KBr pellets of respective metal oxides.

2.1.1 Synthesis of Functionalized Metal Oxide Nanoparticles

In a 50.0 mL round-bottomed flask, metal oxide nanoparticles (50.0 mg) were added to toluene (10.0 mL), followed by 4-formylbenzoic acid (0.5 mmol). The mixture was stirred for 12 h at 60°C. Later, it was centrifuged (3000 rpm) to collect the surface-modified NPs. The functionalized particles were washed with ethanol (3 × 10.0 mL each) to remove unreacted carboxylic acids and oven-dried at 80°C for 12 h to get into powder form. FT-IR characterized the material. Similarly, all surface-modified materials were synthesized (**Scheme 1**). As shown in Figure 3, different organic moieties were used to get surface functionalized materials.

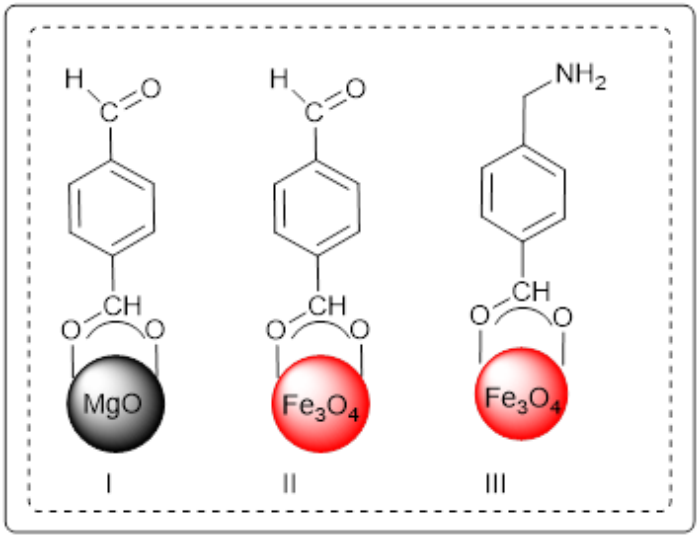

Scheme 1 Surface modified MgO and Fe_3O_4 materials (I, II, III).

2.1.2 Synthesis of Composite Materials

The functionalized metal oxide NPs, either **I and III** or **II** and **III** (as shown in Scheme 1), were stirred in solutions of (1:1 molar equiv.) in ethanol for 12 under a nitrogen atmosphere at 60°C. Later, these particles were centrifuged, washed with ethanol (2 × 10.0 mL), and dried in a vacuum for 12 h to obtain fine powder.

2.1.3 Dehydration of Glucose

Glucose (1.0 mmol) dissolved in 10.0 mL of HPLC water was added to the 50.0 mL round-bottomed flask containing 20.0 mg of NOFs, and stirring was continued at the required temperature. Later, the reaction mixture was centrifuged to separate the catalyst and analyzed by HPLC using C-18 column (MeOH: H_2O, 1:9)

3. Results and Discussion

3.1 FT-IR

All the metal oxide NPs were characterized by FT-IR, which revealed that the surface of NPs was modified. The M-O stretching vibration frequency at nearly 580 cm-1 was observed for freshly prepared metal oxides and also after surface modification (Figure S1-Figure S4). In addition, surface hydroxyls were present at 3300 cm^{-1} on the surface of freshly prepared metal oxides. Notably, the stretching frequency at 1100 cm^{-1} is assigned to the presence of C-C bonds of the modifier (Figure S1-Figure S4). Two characteristic peaks of carboxylic acid bidentate modes appeared at ~1410 cm^{-1} and ~1600 cm^{-1}. It reflects that the carboxylic acid group of 4-formyl benzoic acid and 4-aminomethyl benzoic acids are effectively adsorbed on the surface of metal oxide NPs. Further, the amine-functionalized materials show the stretching frequency of -NH_2 at ~3390 cm^{-1}. It indicates that amine groups are free and carboxylate groups are successfully anchored to the surface of nanometal oxides. Of particular note is that the imine bond formation to the metal oxide NPs of various structures was confirmed from the appearance of weak stretch at ~1620 cm-1 and the broad

stretching frequency at ~3400 cm^{-1} for NOFs A, B, C, and D (Figure 4). This is due to the presence of the secondary amines (-NH) of imine linkage. In addition, peaks at ~2910 cm^{-1} are assigned to be symmetric and asymmetric -CH_2 stretches in the 4-aminomethyl benzoic acid-treated metal oxides (Figure S1 and Figure S2). The C-H and C=C stretching vibration frequencies are also observed at nearly 753 and 1570 $cm^{-1,}$ corresponding to the aromatic group (complete IR data was provided in the supporting information Figure S1-Figure S4).

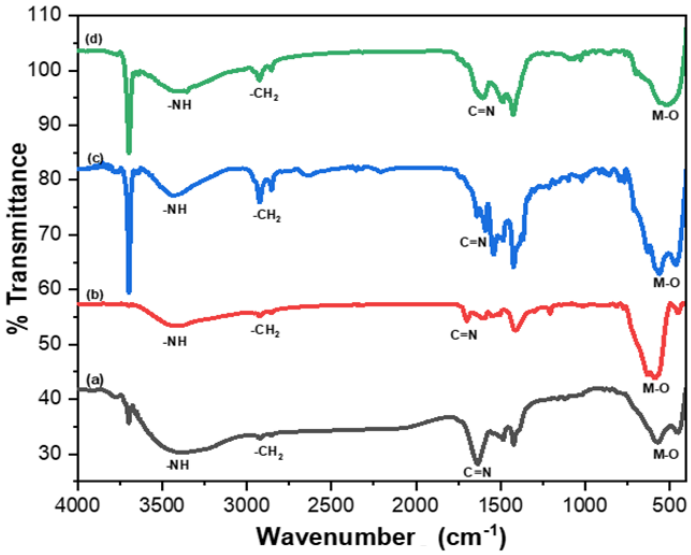

Figure 4 FT-IR spectra of synthesized (a) NOF-A; (b) NOF-B; (c) NOF-C ;(d) NOF-D.

3.2 Powdered X-ray Diffraction (PXRD)

XRD characterized synthesized and surface-modified catalysts' composition and phase purity. The diffraction pattern of freshly prepared iron oxide and magnesium oxide samples shows vast peaks, indicating the small crystallite of particles, 10.7 and 21.5 nm, calculated from the Debye Scherer (DS) equation.

Debye Scherer equation: $D = 0.9\lambda/\beta\ cos\ \theta$ (λ = 1.54 Å), where β is the FWHM (Full Width Half Maximum).

The presence of (220), (311), (422), and (511) revealed the cubic spinel phase of superparamagnetic iron oxide. Further, the presence of (111), (200), and (220) showed the cubic structure of MgO (Figure S5 to Figure S8). It was observed that the intensities of diffraction peaks were consistent with the standard pattern. (The diffraction peaks were comparable to JCPDS (card number for MgO 45-0946 and iron oxide 01-071-6336). Especially in the case of nano MgO when it was modified with 4-formyl benzoic acid (**L1**), the decrease in intensity of (200) plane indicates that organic moiety has interacted with (200) plane and remains intact with other aircraft (Figure 5). The crystallite sizes increased from 10.7 nm to 12.5 and 14.6 nm for surface-modified iron oxides (Table 1, Entries 2 and 4). In contrast, the dimensions of magnesium oxide NPs decreased from 21.5 to 13.1 nm for the surface-modified MgO with 4-formyl benzoic acid (Figure S5 to Figure S7). Remarkably, crystallite size increased to 34.9 nm for (*L*)-phenylalanine adjusted MgO. All the peaks related to iron oxide and magnesium oxide indexed planes were identified in the NOFs (as expected) (Figure 5). Notably, the crystallite sizes of respective composite materials of combined metal oxides are at 11.3, 11.8, 14.1, and 24.0 nm, respectively, for NOFs A, B, C, and D (Table 1). The particle size change

after surface modification is due to metal interaction (Fe or Mg) with organic ligands rather than Fe-Fe or Mg-Mg interactions.

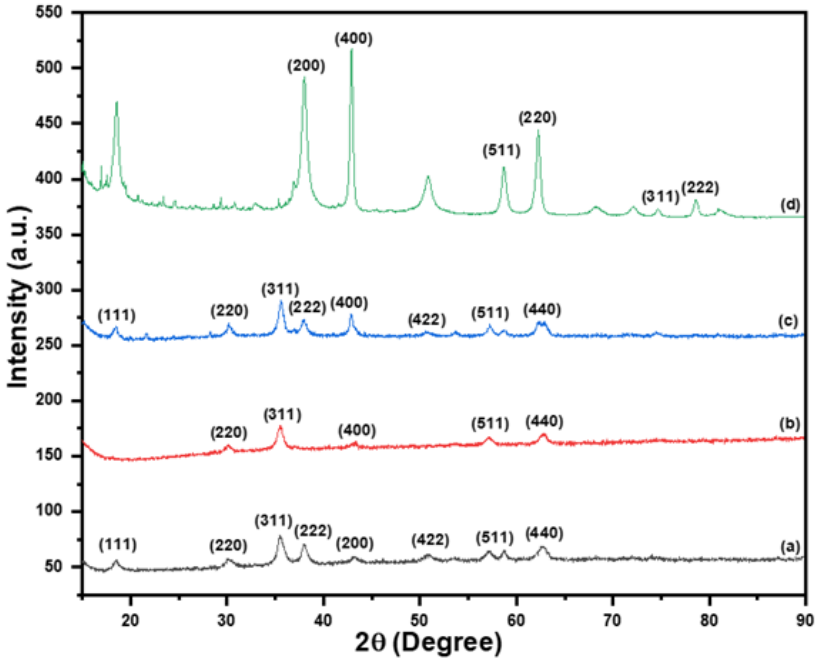

Figure 5 PXRD spectra of (a) NOF-A; (b) NOF-B; (c) NOF-C; (d) NOF-D.

Table 1 Crystallite Sizes of surface-modified NPs.

S.No	Name of the metal oxide	Crystallite Size using DS equation (nm)
1	Fe_3O_4 NPs	10.7
2	Fe_3O_4-modified with L2	12.5
3	Fe_3O_4-modified with L1	14.6
4	MgO NPs	21.5
5	MgO-modified with L2	13.1
6	MgO-modified with L3	34.9
7	NOF-A	11.3
8	NOF-B	11.8
9	NOF-C	14.1
10	NOF-D	24.0

4. Thermal Analysis

The thermal properties of synthesized NOFs were examined by TGA analysis. The non-isothermal curves of NOFs are shown in Figure 6. In the TGA curve of NOFs-A, three weight losses were observed. The initial weight loss up to 265°C was only 8.7% weight loss, which is attributed to the loss of organic molecules from metal oxides. The second weight loss up to 370°C exhibited nearly 9.0%. However, the last decomposition occurred up to 440°C with a weight loss of 15.7%. These two decompositions are attributed to the loss of water molecules associated with two metal oxides. In contrast to NOF-A, NOF-B exhibits only two-step decompositions. The first decomposition step

occurred at 360°C with nearly 5.0% weight loss. The second step in the 360-440°C range exhibited weight loss of approximately 7.0%. Interestingly, in NOF-C, the decomposition of the first step is at 300°C with 7.8% weight loss, which is attributed to the loss of organic molecules. The second step, up to 390°C, exhibited weight loss of nearly 10.0%. However, the last step occurred up to 600°C with a weight loss of almost 18.0%. In the NOF-D, the first decomposition step for the imine complex of NOF-D occurred at 300°C with 6.5% weight loss. In the second step, the 300-600°C range exhibited weight loss of nearly 31%.

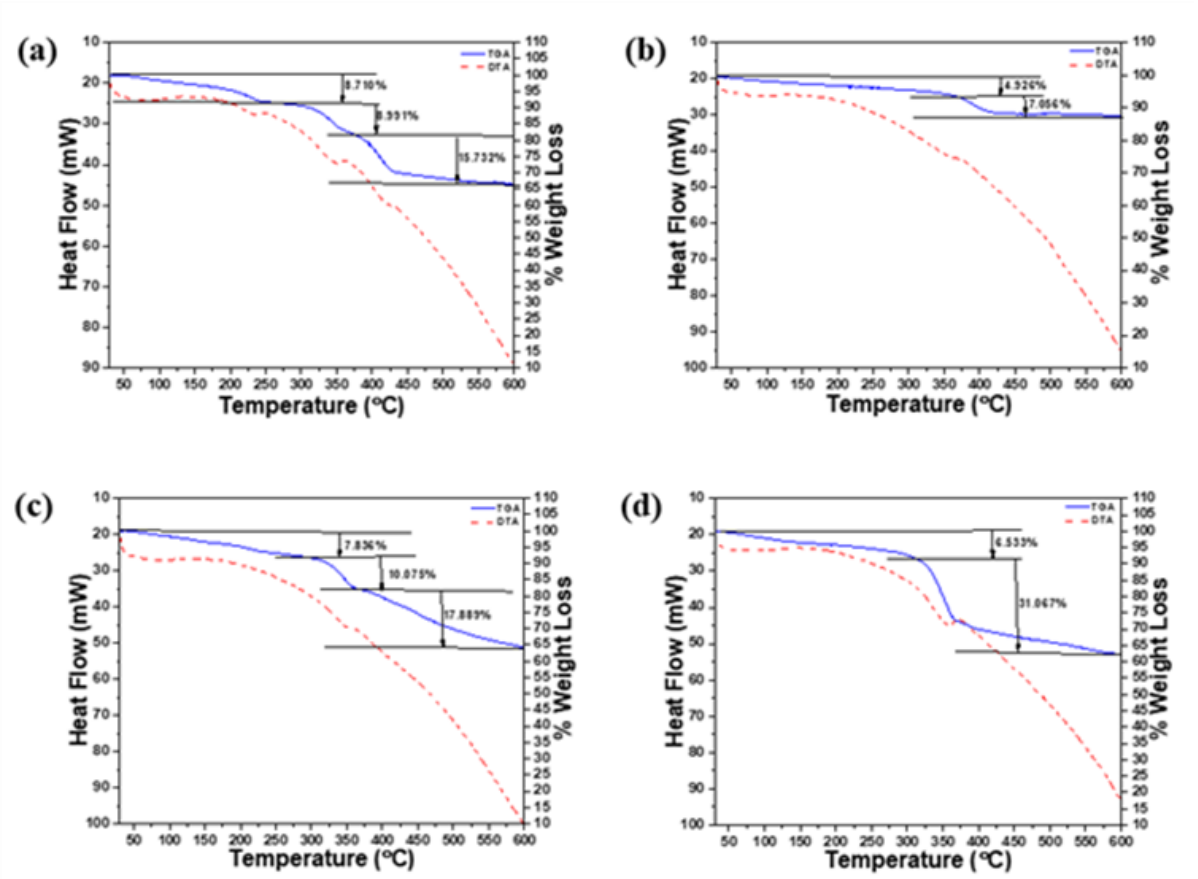

Figure 6 TGA and DTA graph of (a) NOF-A; (b) NOF-B; (c) NOF-C; (d) NOF-D.

It was noticed that when two different metal oxides combined to form NOFs, three decompositions were observed, whereas NOF formation took place with the same metal oxides. Only two decays were observed (Figure 6).

The elemental percentage in the material can be studied using EDS analysis. The EDS graphs of NOF-A, shown in Figure 7A, indicate the presence of Fe, Mg, O, N, and C. The EDS graph confirms the presence of all expected elements with a C: N ratio of 1:2. As expected, NOF-B, C, and D show the elemental composition of respective materials. Within a mapped area of each sample, a heterogeneous distribution for most of the elements Fe, Mg, C, N, and O is evident.

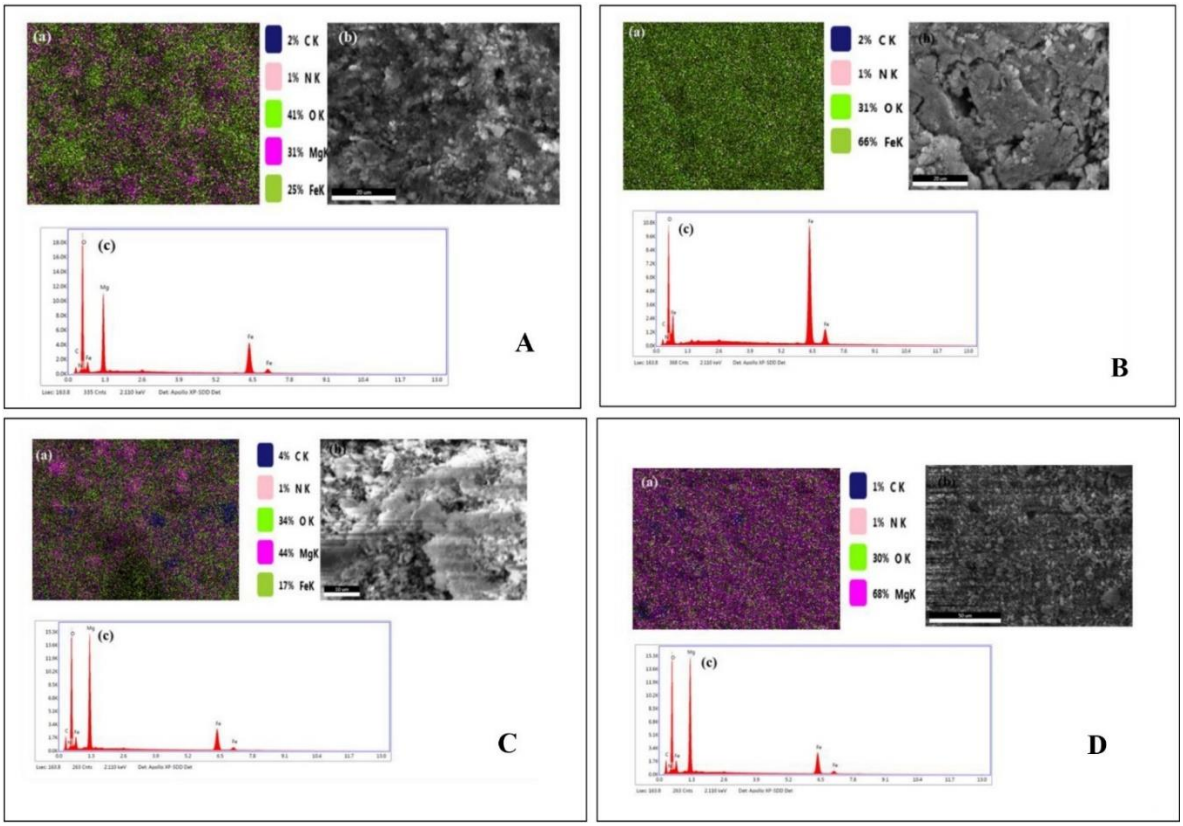

Figure 7 Elemental mapping, SEM-EDX of (a) NOF-A; (b) NOF-B; (c) NOF-C; (d) NOF-D.

Further, these composite materials have been evaluated in the degradation/dehydration of glucose at various temperatures in the presence of aqueous medium. It was found that furan derivatives such as 5-hydroxymethylfurfural (HMF) and diformylfuran (DFF) were obtained in good yields in organic-inorganic hybrid materials. These furan derivatives are value-added components for the synthesis of biobased fuels and also in plastic technology. Surface modification of metal oxides has been successfully used in decomposing either fructose or glucose, and our present results were comparable to earlier reported results [16-22]. The significant byproducts formed during the dehydration of carbohydrates are levulinic acid and its derivatives [23, 24].

Various catalysts have been used to determine the best motivation for dehydrating biomass-derived glucose. Pure magnesium oxide was used, and iron oxide did not show any conversion in the dehydration reactions (Table 2, Entries 1, 2, 4). Increasing the temperature also produced meager HMF yields without DFF formation. Surface modification of MgO with L1 and Fe_3O_4 with L2 and L3 also did not affect glucose conversion to furan derivatives (Table 2, Entries 3, 5, 6). However, 5-HMF formed selectively has been used for the dehydration of glucose in an aqueous solution selectively after 24 h at room temperature when catalyzed by NOF "A." Remarkably, at 80°C it subsequently oxidized to DFF in a short period (Table 2, Entries 7, 8 and 9). NOF "B" is highly active in producing DFF in good yields up to 96%. The higher reactivity may be due to the same metal oxides (magnetite NPs), which facilitates the dehydration reaction more quickly than when two different metal oxides. When NOF "C" was used for the dehydration of glucose at 80°C, a mixture of both HMF and DFF was obtained. Noticeably, in the presence of NOF "D," HMF was obtained as only the product in 95% yield after 6 h at 80°C (Table 2, Entries 10, 11).

Table 2 Dehydration of glucose using various catalysts.

S.No	Catalyst	Temp (°C)	Time (h)	HMF	DFF
1	MgO	RT	24		-
2	MgO	80	24		-
3	Surface-modified MgO with L1	80	24	18	-
4	Fe_3O_4	80	24		-
5	Surface modified Fe_3O_4 with L2	80	24	15	-
6	Surface modified Fe_3O_4 with L3	80	24		-
7	NOF-A	RT	24	99%	-
8	NOF-A	80	6	5	90[a]
9	NOF-B	80	6	-	96[a]
10	NOF-C	80	6	50	39[a]
11	NOF-D	80	6	95	-

Reaction conditions: NOFs (20.0 mg), glucose (1.0 mmol), HPLC water (10.0 mL); [a]: Reaction carried out in the presence of air.

The obtained results with NOFs are comparable with the literature-reported values and even superior to some heterogeneous catalysts (as shown in Table 3). In general surface, modified catalysts are highly active in dehydration reactions, and this work attempted to prepare NOFs by combining two different metal oxides through a linker. Our catalysts show good catalytic activity under heterogeneous conditions (Table 3, Entry 27).

Table 3 Comparison of our catalytic data with reported literature values.

Entry	Catalyst	Temp (°C)	Solvent	Time (min)	Conversion (%)	Selectivity (HMF) (%)	Reference (main text)
1	Sulfonic acid-functionalized MOF	120	DMSO	60	99	91	**[25]**
2	Aluminium doped zirconium phosphate	135	Water	240	12	40	**[26]**
3	Niobium catalysts	120	Water	180	92	52	[27]
4	Sulfated zirconia	180	Acetone/DMSO	5	93	73	[28]
5	Sulfonic acid functionalized silica	100	DMSO	60	75	54	[29]
6	Solid silica immobilized ionic liquid	100 (MW)	DMSO	4	100	74	[30]
7	SnO_2–ZrO_2	120	DMSO	150	--	75	[31]
8	WO_3/ZrO_2	130	water	240	60	40	[32]
9	Sn-W oxide	80	DMSO	720	99	70	[33]
11	Dowex-type ion-exchange resin	110	DMSO	300	100	85	[34]
12	Ion exchange resin	90	Water/MIBK	1080	98	85	[35]

13	Dowex-type ion-exchange resin	150	water	60	82	34	[36]
15	Dowex-type ion-exchange resin	150 (MW)	Acetone/DMSO	30	99.4	82	[37]
16	Amberlyst 15 pellets	120	DMSO	120	100	92	[38]
17	Amberlyst 15	80	[BMIM][Cl]	10	98.6	83.3	[39]
18	HT/Amberlyst 15	100	DMF	180	99	76	[40]
19	Amberlyst 15	80	[BMIM][PF6]/DMSO	1440	--	80	[41]
20	12-MPA	120	[BMIM][Cl]/acetonitrile	180	99	98	[42]
21	Functionalized CNTs	80	DMF	480	75	99	[43]
22	Mg-NHCs	100	DMF	120	99	89	[13]
23	Surface modified ferrites	80	Solvent-free	60	96	89	[14]
24	Carbon particles on magnetite	80	Water	18 h	90	99	[20]
25	Polyhexahydrotriazine	80	Water	24 h	99	23	[44]
26	V_2O_5/Vulcan X	100	Water	16 h	90	98	[45]
27	**NOFs (This work)**	RT-80	Water	6-24 h	95-99% yield		

The recyclability of NOF-A has been tested in the dehydration of glucose at room temperature. It was found that the catalyst could be recycled five times with minor changes in the activity. These results indicate that our motivation is highly stable and robust. To the best of our knowledge, molecular welding of two metal oxides was reported for the first time (Table 4).

Table 4 Recyclability of NOF-A catalyzed dehydration of glucose at room temperature.

S.No	Cycle	Temp (°C)	Time (h)	HMF	DFF
1	1	RT	24	99%	-
2	II	RT	24	85	-
3	III	RT	36	90	-
4	IV	RT	36	82	12
5	V	RT	36	80	15

Reaction conditions: NOFs (20.0 mg), glucose (1.0 mmol), HPLC water (10.0 mL)

The plausible mechanism for the formation of furan derivatives through the degradation of glucose is shown in the figure. Hydrogen bonding interactions could have occurred with cavities of metal oxide welding materials. Moreover, both metal oxides are essential and, therefore, decomposed to the formation of furan derivatives in high yields (Figure 8).

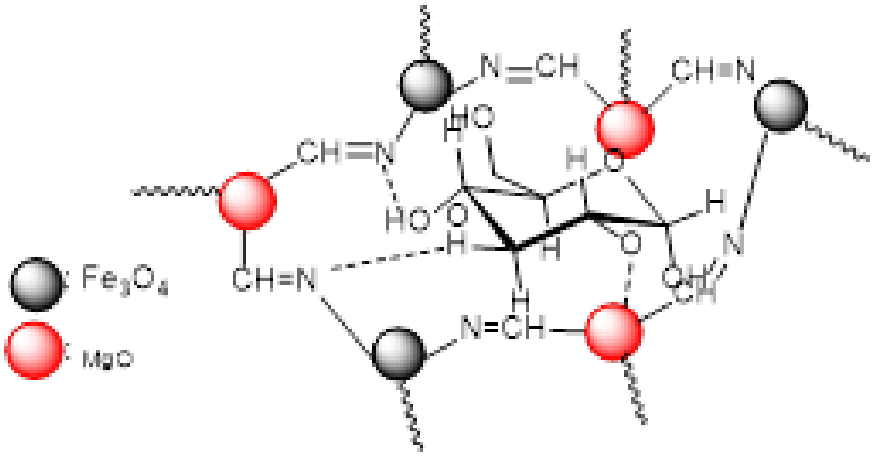

Figure 8 shows plausible interactions of NOF with glucose and subsequently dehydration into products.

5. Conclusion

The surface modification of magnesium and iron oxide NPs has been carried out and characterized using various techniques. The coupling of these two metal oxide NPs leads to forming organic-inorganic hybrid material. These inorganic nanohybrid materials lead to the formation of NOFs. Thus, characterized NOFs are active in the dehydration of biomass-derived glucose to 5-HMF in high selectivity and, subsequently, the oxidation of HMF to DFF. These two furan compounds are highly valuable intermediates in the synthesis of biofuels.

Acknowledgments

Authors would like to thank Institute of Eminence (IoE-6031), Banaras Hindu University, Varanasi for providing the financial grant. Authors also thank to CSIR for providing financial support.

Author Contributions

Ms. Rama Jaiswal was involved in the synthesis of nanomaterials. Dr. Melad Shaikh was extensively studied dehydration of glucose. Dr. Kalluri VS Ranganath involved in providing the scheme, monitoring, writing.

Competing Interests

The authors have declared that no competing interests exist.

Additional Materials

The following additional materials are uploaded at the page of this paper.

1. FT-IR, PXRD, TGA and HPLC spectra of various catalysts are placed in supporting information. HPLC spectra of different catalytic reactions are also placed in revised manuscript.

References

1. Portilla L, Halik M. Smoothly tunable surface properties of aluminum oxide core–shell nanoparticles by a mixed-ligand approach. ACS Appl Mater Interfaces. 2014; 6: 5977-5982.
2. Al-Shatty W, Alexander S, Barron AR. Stability of carboxylic acid modified alumina nanoparticles for enhanced oil recovery and applications. AIP Conf Proc. 2023; 2643: 060015.
3. Barron AR. The interaction of carboxylic acids with aluminium oxides: Journeying from a basic understanding of alumina nanoparticles to water treatment for industrial and humanitarian applications. Dalton Trans. 2014; 43: 8127-8143.
4. Neouze MA, Schubert U. Surface modification and functionalization of metal and metal oxide nanoparticles by organic ligands. Monatsh Chem. 2008; 139: 183-195.
5. Pujari SP, Scheres L, Marcelis AT, Zuilhof H. Covalent surface modification of oxide surfaces. Angew Chem Int Ed. 2014; 53: 6322-6356.
6. Ganapathe LS, Mohamed MA, Mohamad Yunus R, Berhanuddin DD. Magnetite (Fe_3O_4) nanoparticles in biomedical application: From synthesis to surface functionalisation. Magnetochemistry. 2020; 6: 68.
7. Liu S, Yu B, Wang S, Shen Y, Cong H. Preparation, surface functionalization and application of Fe_3O_4 magnetic nanoparticles. Adv Colloid Interface Sci. 2020; 281: 102165.
8. Turcheniuk K, Tarasevych AV, Kukhar VP, Boukherroub R, Szunerits S. Recent advances in surface chemistry strategies for the fabrication of functional iron oxide based magnetic nanoparticles. Nanoscale. 2013; 5: 10729-10752.
9. Ramirez E, Jansat S, Philippot K, Lecante P, Gomez M, Masdeu-Bultó AM, et al. Influence of organic ligands on the stabilization of palladium nanoparticles. J Organomet Chem. 2004; 689: 4601-4610.
10. Woehrle GH, Hutchison JE. Thiol-functionalized undecagold clusters by ligand exchange: Synthesis, mechanism, and properties. Inorg Chem. 2005; 44: 6149-6158.
11. Alexander S, Morrow L, Lord AM, Dunnill CW, Barron AR. pH-responsive octylamine coupling modification of carboxylated aluminium oxide surfaces. J Mater Chem A. 2015; 3: 10052-10059.
12. Alexander S, Gomez V, Barron AR. Carboxylation and decarboxylation of aluminum oxide nanoparticles using bifunctional carboxylic acids and octylamine. J Nanomater. 2016; 2016: 7950876.
13. Shaikh M, Sahu M, Khilari S, Kumar AK, Maji P, Ranganath KV. Surface modification of polyhedral nanocrystalline MgO with imidazolium carboxylates for dehydration reactions: A new approach. RSC Adv. 2016; 6: 82591-82595.
14. Shaikh M, Sahu M, Atyam KK, Ranganath KV. Surface modification of ferrite nanoparticles with dicarboxylic acids for the synthesis of 5-hydroxymethylfurfural: A novel and green protocol. RSC Adv. 2016; 6: 76795-76801.
15. Climent MJ, Corma A, Iborra S. Converting carbohydrates to bulk chemicals and fine chemicals over heterogeneous catalysts. Green Chem. 2011; 13: 520-540.
16. Jiang Z, Zeng Y, Hu D, Guo R, Yan K, Luque R. Chemical transformations of 5-hydroxymethylfurfural to highly added value products: Present and future. Green Chem. 2022; 25: 871-892.

17. Takagaki A, Takahashi M, Nishimura S, Ebitani K. One-pot synthesis of 2,5-diformylfuran from carbohydrate derivatives by sulfonated resin and hydrotalcite-supported ruthenium catalysts. ACS Catal. 2011; 1: 1562-1565.
18. Zhong X, Yuan P, Sadjadi S, Liu D, Wei Y. Palygorskite-supported ruthenium catalysts for the efficient selective oxidation of 5-hydroxymethylfurfural to 2,5-diformylfuran. Appl Clay Sci. 2023; 242: 107023.
19. Sarmah B, Satpati B, Srivastava R. One-pot tandem conversion of monosaccharides and disaccharides to 2,5-diformylfuran using a Ru nanoparticle-supported H-beta catalyst. Catal Sci Technol. 2018; 8: 2870-2882.
20. Jaiswal R, Ranganath KV. Carbon nanoparticles on magnetite: A new heterogeneous catalyst for the oxidation of 5-hydroxymethylfurfural (5-HMF) to 2,5-diformoylfuran (DFF). J Inorg Organomet Polym Mater. 2021; 31: 4504-4511.
21. Shaikh M, Sahu M, Gavel PK, Turpu GR, Khilari S, Pradhan D, et al. Mg-NHC complex on the surface of nanomagnesium oxide for catalytic application. Catal Commun. 2016; 84: 89-92.
22. Yang Z, Qi W, Su R, He Z. Selective synthesis of 2,5-diformylfuran and 2,5-furandicarboxylic acid from 5-hydroxymethylfurfural and fructose catalyzed by magnetically separable catalysts. Energy Fuels. 2017; 31: 533-541.
23. Qi L, Mui YF, Lo SW, Lui MY, Akien GR, Horváth IT. Catalytic conversion of fructose, glucose, and sucrose to 5-(hydroxymethyl) furfural and levulinic and formic acids in γ-valerolactone as a green solvent. ACS Catal. 2014; 4: 1470-1477.
24. Wu D, Hakkarainen M. A closed-loop process from microwave-assisted hydrothermal degradation of starch to utilization of the obtained degradation products as starch plasticizers. ACS Sustain Chem Eng. 2014; 2: 2172-2181.
25. Chen J, Li K, Chen L, Liu R, Huang X, Ye D. Conversion of fructose into 5-hydroxymethylfurfural catalyzed by recyclable sulfonic acid-functionalized metal–organic frameworks. Green Chem. 2014; 16: 2490-2499.
26. Ordomsky VV, Schouten JC, van der Schaaf J, Nijhuis TA. Zirconium phosphate coating on aluminum foams by electrophoretic deposition for acidic catalysis. ChemCatChem. 2012; 4: 129-133.
27. Nakajima K, Baba Y, Noma R, Kitano M, Kondo JN, Hayashi S, et al. $Nb_2O_5{\cdot}nH_2O$ as a heterogeneous catalyst with water-tolerant Lewis acid sites. J Am Chem Soc. 2011; 133: 4224-4227.
28. Yan H, Yang Y, Tong D, Xiang X, Hu C. Catalytic conversion of glucose to 5-hydroxymethylfurfural over SO_4^{2-}/ZrO_2 and $SO_4^{2-}/ZrO_2–Al_2O_3$ solid acid catalysts. Catal Commun. 2009; 10: 1558-1563.
29. Hu L, Tang X, Wu Z, Lin L, Xu J, Xu N, et al. Magnetic lignin-derived carbonaceous catalyst for the dehydration of fructose into 5-hydroxymethylfurfural in dimethylsulfoxide. Chem Eng J. 2015; 263: 299-308.
30. Bao Q, Qiao K, Tomida D, Yokoyama C. Preparation of 5-hydroymethylfurfural by dehydration of fructose in the presence of acidic ionic liquid. Catal Commun. 2008; 9: 1383-1388.
31. Wang Y, Tong X, Yan Y, Xue S, Zhang Y. Efficient and selective conversion of hexose to 5-hydroxymethylfurfural with tin–zirconium-containing heterogeneous catalysts. Catal Commun. 2014; 50: 38-43.

32. Kourieh R, Rakic V, Bennici S, Auroux A. Relation between surface acidity and reactivity in fructose conversion into 5-HMF using tungstated zirconia catalysts. Catal Commun. 2013; 30: 5-13.
33. Yamaguchi K, Sakurada T, Ogasawara Y, Mizuno N. Tin–tungsten mixed oxide as efficient heterogeneous catalyst for conversion of saccharides to furan derivatives. Chem Lett. 2011; 40: 542-543.
34. Halliday GA, Young RJ, Grushin VV. One-pot, two-step, practical catalytic synthesis of 2,5-diformylfuran from fructose. Org Lett. 2003; 5: 2003-2005.
35. Chheda JN, Dumesic JA. An overview of dehydration, aldol-condensation and hydrogenation processes for production of liquid alkanes from biomass-derived carbohydrates. Catal Today. 2007; 123: 59-70.
36. Qi X, Watanabe M, Aida TM, Smith Jr RL. Catalytic dehydration of fructose into 5-hydroxymethylfurfural by ion-exchange resin in mixed-aqueous system by microwave heating. Green Chem. 2008; 10: 799-805.
37. Bicker M, Hirth J, Vogel H. Dehydration of fructose to 5-hydroxymethylfurfural in sub-and supercritical acetone. Green Chem. 2003; 5: 280-284.
38. Yi G, Teong SP, Li X, Zhang Y. Purification of biomass‐derived 5-hydroxymethylfurfural and its catalytic conversion to 2, 5-furandicarboxylic acid. ChemSusChem. 2014; 7: 2131-2135.
39. Hu S, Zhang Z, Zhou Y, Song J, Fan H, Han B. Direct conversion of inulin to 5-hydroxymethylfurfural in biorenewable ionic liquids. Green Chem. 2009; 11: 873-877.
40. Zhou J, Xia Z, Huang T, Yan P, Xu W, Xu Z, et al. An ionic liquid–organics–water ternary biphasic system enhances the 5-hydroxymethylfurfural yield in catalytic conversion of glucose at high concentrations. Green Chem. 2015; 17: 4206-4216.
41. Swift TD, Nguyen H, Anderko A, Nikolakis V, Vlachos DG. Tandem Lewis/Brønsted homogeneous acid catalysis: Conversion of glucose to 5-hydoxymethylfurfural in an aqueous chromium (III) chloride and hydrochloric acid solution. Green Chem. 2015; 17: 4725-4735.
42. Ranoux A, Djanashvili K, Arends IW, Hanefeld U. 5-Hydroxymethylfurfural synthesis from hexoses is autocatalytic. ACS Catal. 2013; 3: 760-763.
43. Ranganath KV, Sahu M, Shaikh M, Gavel PK, Atyam KK, Khilari S, et al. $CoFe_2O_4$-decorated carbon nanotubes for the dehydration of glucose and fructose. New J Chem. 2016; 40: 4468-4471.
44. Rai A, Jaiswal R, Pandey M, Ranganath KV. High performance Polyhexahydrotriazine (PHT) thermoset for the synthesis of furanics. BioEnergy Res. 2023; 16: 507-516.
45. Pandey M, Gupta PK, Jaiswal R, Ranganath KV. Synthesis of value-added furan compounds from biomass derived glucose via cascade catalysis using functionalized V_2O_5 catalysts. Inorg Chem Commun. 2022; 146: 110226.